

Localization of corresponding points in fingerprints by complex filtering

Kenneth Nilsson, Josef Bigun

School of Information Science, Computer and Electrical Engineering (IDE)

Halmstad University, P.O. Box 823, SE-301 18 Halmstad, Sweden.

Kenneth.Nilsson@ide.hh.se, Josef.Bigun@ide.hh.se

Abstract

For the alignment of two fingerprints certain landmark points are needed. These should be automatically extracted with low misidentification rate. As landmarks we suggest the prominent symmetry points (singular points, SPs) in the fingerprints. We identify an SP by its symmetry properties. SPs are extracted from the complex orientation field estimated from the global structure of the fingerprint, i.e. the overall pattern of the ridges and valleys. Complex filters, applied to the orientation field in multiple resolution scales, are used to detect the symmetry and the type of symmetry. Experimental results are reported.

1 Introduction

A fingerprint image can be said to have two structures, the global structure and the local structure. By the global structure we mean the overall pattern of the ridges and valleys, and the local structure the detailed patterns around a minutiae point (a position in the fingerprint where a ridge is suddenly broken or two ridges are merged).

Direct use of the local structure in the identification/verification process is sensitive to noise, i.e. poor performance for low quality fingerprints can be foreseen. Compared to the local structure the global structure is more stable even when the fingerprint is of poor quality [1].

Here we suggest to first align the reference and the

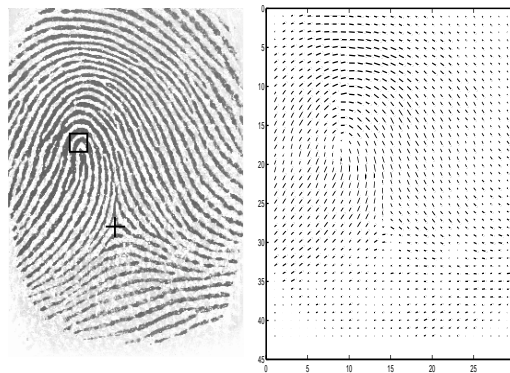


Figure 1: Left: marked singular points, a core point is marked with a square and a delta point with a cross. Right: the estimated orientation field at level 3.

unknown fingerprint before using the local structure for the identification/verification. In this alignment the global structure of the fingerprint is used. When the two fingerprints are aligned (registered) we can match the local structure for certain points on the basis of the neighborhood content more robustly than by extracting minutiae positions and matching on the basis of the geometric position distribution of the minutiae.

For the alignment we need certain landmark points (singular points, SPs) in the fingerprint that are less prone to misidentification. Typical SPs (core and delta points) are shown in Figure 1. As can be seen

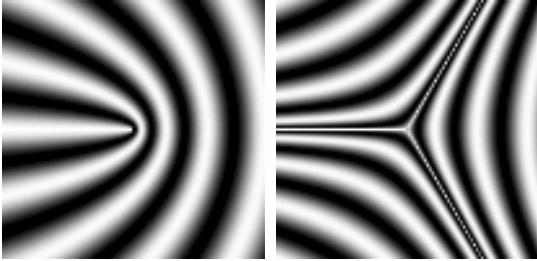


Figure 2: Patterns with a local orientation description of $z = \exp\{i\varphi\}$ (left) and $z = \exp\{-i\varphi\}$ (right).

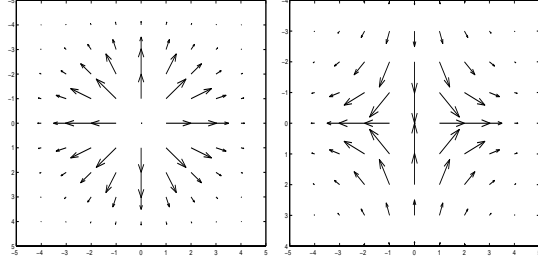


Figure 3: Left: filter h_1 , detects "core-type" symmetry. Right: filter h_2 , detects "delta-type" symmetry.

these points have special symmetry properties which make them easy to identify also by humans. We identify an SP by its symmetry properties, i.e. its strong response to complex filters designed for rotational symmetry extraction.

Two different filters are used, one for the "core type" and one for the "delta type" symmetry. The filtering is applied to complex images, i.e. the orientation tensor field [2] in different scales. The orientation tensor field is often used to represent the global structure in a fingerprint [3, 1, 4]. Also when estimating curvature in oriented patterns the orientation field is used [5, 6]. An original fingerprint and its estimated orientation field are shown in Figure 1 as illustration.

A common technique to extract SPs (core and delta points) in fingerprints is to use the *Poincaré index* introduced by Kawagoe and Tojo [7]. The *Poincaré index* takes the values 180° , -180° , and 0° for a core point, a delta point, and an ordinary point respectively. It is obtained by summing the change in orientation following a closed curve counterclockwise around a point [3]. This technique has been used in the work of Karu and Jain [3], and Bazen and Gerez [8] to define and extract SPs.

Our method using complex filters compared to *Poincaré index* to identify SPs has the advantage to extract not only the position of an SP but also its spatial orientation. When two fingerprints are rotated and translated relative to each other our method can estimate both translation and rotation parameters at once. In the work of Bazen and Gerez [8] the position

extraction and the orientation estimation of an SP is done in two sequential steps. The position extraction is performed by using *Poincaré index*. The orientation estimation is done by matching a reference model of the orientation field around an SP with the orientation map of the extracted SP obtained by using a technique introduced in [2, 9, 10, 11].

This paper presents the theory and experimental results for automatic extraction of SPs including their spatial orientation from the global structure using complex filters designed to detect rotational symmetries.

2 Symmetry point extraction

2.1 Filters for rotational symmetry detection

Complex filters, of order m , for the detection of patterns with radial symmetries are modelled by $\exp\{im\varphi\}$ [9, 12, 11]. A polynomial approximation of these filters in gaussian windows yields $(x + iy)^m g(x, y)$ where g is a gaussian defined as $g(x, y) = \exp\{-\frac{x^2+y^2}{2\sigma^2}\}$ [13]. A gaussian is used as window because the gaussian is the only function which is orientation isotropic (in polar coordinates, it is a function of radius only) and separable [14]. In image analysis this translates to that all filters which are separable introduce orientation dependent bias if they are not gaussians. For a review of the properties of gaussians relevant to image analysis we refer to [13].

It is worth to note that these filters are not applied to the original fingerprint image but instead they are applied to the complex valued orientation tensor field image $z(x, y) = (f_x + if_y)^2$. Here f_x is the derivative of the original image in the x-direction and f_y is the derivative in the y-direction.

In our experiments we use filters of first order symmetry or parabolic symmetry i.e.

$$h_1(x, y) = (x + iy)g(x, y) = r \exp\{i\varphi\}g(x, y) \text{ and}$$

$$h_2 = (x - iy)g(x, y) = r \exp\{-i\varphi\}g(x, y).$$

Patterns that have a local orientation description of $z = \exp\{i\varphi\}$ (m=1) and $z = \exp\{-i\varphi\}$ (m=-1) are shown in Figure 2. As can be seen these patterns are similar to patterns of a core respectively a delta point in a fingerprint and therefore suitable to use as SP-extractors. Figure 3 shows the complex filter h_1 and h_2 respectively.

The complex filter response is $c = \mu \exp\{i\alpha\}$, where μ is a certainty measure of symmetry, and α is the "member" of that symmetry family, here represented by the geometric orientation of the symmetric pattern. By using the certainty measures μ_1 and μ_2 for core point respectively delta point symmetry, we can identify an SP of type core if $|\mu_1| > T_1$ and of type delta if $|\mu_2| > T_2$, where T_1 and T_2 are thresholds.

2.2 Multi-scale filtering

Using a multi-resolution representation of the complex orientation field offers a possibility to extract SPs more robustly and precisely compared to a representation at only one resolution level. The extraction of an SP starts at the lowest resolution level (a smooth orientation field) and continues with refinement at higher resolutions. The result at a low resolution guides the extraction at higher resolution levels.

Drets and Liljenstrom [15] points out that the pattern of the orientation field around core and delta points are the same at different resolution levels. This means that the same SP-extractor can be used for all scales. As an SP-extractor we use complex filters compared to Drets and Liljenstrom who used a sliding neural network that require training.

The complex orientation field $z(x, y)$ is represented

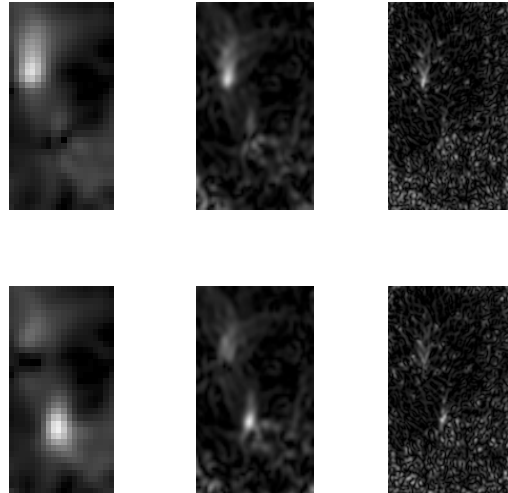


Figure 4: Row1: filter response μ_{1k} , k=3, 2, and 1. Row2: filter response μ_{2k} , k=3, 2, and 1.

by a four level gaussian pyramid. Level 3 has the lowest, and level 0 has the highest resolution. We only use the angle of the complex orientation field, i.e. the magnitude is set to one in $z(x, y)$ in the multiscale filtering. The core and the delta filtering is applied on each resolution. The complex filter response is called c_{nk} , where k=3, 2, 1 and 0 are the resolution levels, and n=1, 2 are the filter types (core and delta).

Figure 4 shows the magnitude of the filter responses of filter h_1 (called μ_{1k}), and h_2 (called μ_{2k}) for levels k=3, 2, and 1. The filters are applied to the image in Figure 1.

2.3 Maximum filter response

In order to improve the selectivity of the filters, i.e. a filter should give a strong response only to one of the symmetries (here: h_1 to "core type" symmetry and h_2 to "delta type" symmetry) we use the following rules to sharpen the magnitude of the filter responses [16]:

$$\begin{cases} s_{1k} = \mu_{1k}(1 - \mu_{2k}) \\ s_{2k} = \mu_{2k}(1 - \mu_{1k}) \end{cases} \quad (1)$$

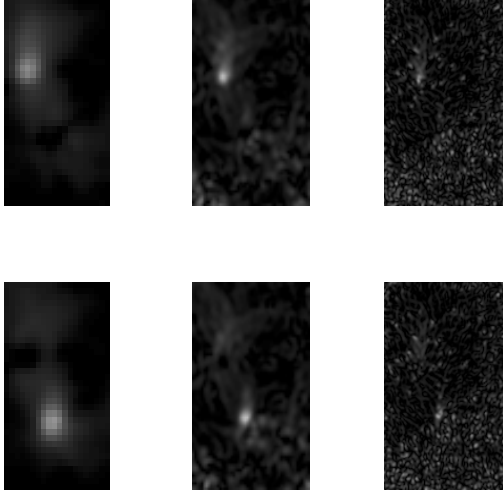


Figure 5: Row1: filter response s_{1k} , $k=3, 2,$ and 1 . Row2: filter response s_{2k} , $k=3, 2,$ and 1 .

with (levels) $k=0, 1, 2,$ and 3 . Figure 5 shows the responses s_{1k} , and s_{2k} .

The complex filter response is now $c_{nk} = s_{nk} \exp\{i\alpha_{nk}\}$, where s_{nk} is a measure of certainty for that there is a symmetry of type n at resolution k , and α_{nk} tells how much the symmetric pattern is rotated compared to a fixed reference.

To find the position of a possible SP in a fingerprint the maximum filter response is extracted in image s_{13} and in s_{23} (level 3). To get even further precision in the localization of the maximum a new search is done in lower levels of the pyramid i.e. in s_{n2} , s_{n1} , and s_{n0} for both $n=1, 2$. The search is done in a window computed in the previous higher level (lower resolution).

At a certain resolution (level k), if $s_{nk}(x_j, y_j)$ is higher than a threshold an SP is found and its position (x_j, y_j) and the complex filter response $c_{nk}(x_j, y_j)$ are noted.

3 Alignment

We assume that two fingerprints are rotated and translated relative to each other, i.e. an Euclidian

transformation. This model is parameterized by a rotation angle φ and a translation vector $v = (v_x, v_y)^t$ [17].

A point $p = (x, y)^t$ in image 1 is transformed to a point $p' = (x', y')^t$ in image 2 by:

$$(p' - p_{rot}) = Q(p - p_{rot}) + v \quad (2)$$

Where Q is the 2 by 2 rotation matrix:

$$Q = \begin{pmatrix} \cos\varphi & \sin\varphi \\ -\sin\varphi & \cos\varphi \end{pmatrix} \quad (3)$$

and $p_{rot} = (x_{rot}, y_{rot})^t$ is the rotation centre.

In this work the transformation parameters are estimated from the correspondence established identifying p and p' which are SPs of the same type in two fingerprint images. This is achieved by matching $s_{nk}(x, y)$ and $s'_{nk}(x', y')$ as well as by finding the spatial orientation of the corresponding symmetric patterns via $\alpha_{nk}(x, y)$ and $\alpha'_{nk}(x', y')$. The translation vector v can be estimated as $v = p' - p$ when the point p is assumed to be the rotation centre with $p_{rot} = p$, and the rotation angle φ is $[\alpha'_{nk}(x', y') - \alpha_{nk}(x, y)]/2$. Division by two is needed because of the double angle representation used in the complex orientation image z to assure continuity in the angle of the orientation tensor [11, 18].

4 Implementation

The 2D scalar product $\langle h, z \rangle$ is calculated for each image point, where $h = (x + iy)^m g(x, y)$ is the complex filter of order m , and z is the complex orientation field, i.e. this is a 2D complex convolution between the image z and the filter h . Due to the separable property of a 2D gaussian function, the filter h can be written as: $h = (x + iy)^m g(x)g(y)$.

The 2D convolution is computed by using several 1D convolutions. A faster implementation can then be achieved.

This is now shown in detail only for a first and second order filter. First order filter:

$$h = (x + iy)g(x)g(y) = xg(x)g(y) + i[yg(y)g(x)].$$

Second order filter:

$$h = (x + iy)^2 g(x)g(y) = (x^2 - y^2 + i2xy)g(x)g(y) = x^2g(x)g(y) - y^2g(y)g(x) + i2[xg(x)yg(y)].$$

By designing the 1D filters $g(t)$, $tg(t)$, and $t^2g(t)$ the filtering of the image z can be performed as:
 $g(y) * ((xg(x))^t * z(x, y)) + ig(x)^t * ((yg(y)) * z(x, y))$
for the first order filters and
 $g(y) * ((x^2g(x))^t * z(x, y)) - g(x)^t * ((y^2g(y)) * z(x, y))$
 $+ i2[(yg(y)) * ((xg(x))^t * z(x, y))]$ for the second order filters. The symbol $*$ represents the convolution operation.

Also in computing the orientation field z , 1D convolutions are used instead of a 2D convolution. This is possible as the derivative filters used are the first partial derivatives of a 2D gaussian function and therefore separable. For further details on derivatives of gaussians in complex fields we refer to [13].

5 Experiments

The FVC2000 fingerprint database, DB2 set A is used in the experiments [19]. A total of 800 fingerprints (100 persons, 8 fingerprint/person) are captured using a low cost capacitive sensor. The size of an image is 364 x 256 pixels, and the resolution is 500 dpi. It is worth to note that FVC2000 is constructed for the purpose of grading the performance of fingerprint recognition systems, and contains many poor quality fingerprints.

5.1 Symmetry point extraction

Only filters of the first order ($m=1$, and $m=-1$) have been used in this work, as these two filters were capable to detect the different types of SPs (core and delta) that is found in fingerprints.

The orientation tensor field $z(x, y) = (f_x + if_y)^2$ has been computed by using a $\sigma = 0.8$. A small value on σ is chosen because we wanted to capture fine details in the fingerprint. We represent the orientation field z using a gaussian pyramid in four levels. Level 3 has the lowest resolution 42 x 28, level 2: 87 x 60, level 1: 178 x 124, and level 0: 360 x 252. A $\sigma = 0.8$ is used in the smoothing before downsampling by 2. In level 3 we have a smooth orientation field that captures the global structure in the fingerprint, see Figure 1 right.

Complex filtering for symmetry detection is done in each level by using 1D filters (g , tg with $\sigma = 1.5$) in x and y directions. As explained in Section 4 this results in efficient computations.

For level 3 only, we compute a modified complex filter response because at this level we obtain an approximative position of the SP which allows further refinement. The level is empirically determined and is kept unchanged for a given fingerprint scanner type. This is done in two steps. Firstly, we locally downweight c_{n3} if a point has low orientation certainty via $c_{n3} \cdot (g_1 * |z_3|)$ where g_1 is a gaussian function with $\sigma = 1.5$ and \cdot is pointwise multiplication. This step downweights the low certainty orientation areas of the image. Secondly, we pointwise multiply a large gaussian which is 1 at the centre and decreases significantly towards the border via $c_{n3} \cdot g_2$ with g_2 having standard deviations as one third of the height of c_{n3} ($=11.7$) and one third of the width of c_{n3} ($=7.0$). This step downweights the border regions of the fingerprint image. Next, these two complex images are averaged according to:

$$c_{n3} \leftarrow 0.5(c_{n3} \cdot (g_1 * |z_3|) + c_{n3} \cdot g_2) \quad (4)$$

so that points with high quality orientation close to the image border (and elsewhere) are not suppressed while border points are generally suppressed due to the low image quality induced by low mechanical pressure at the fingerprint frontiers. The result is reassigned to c_{n3} .

After the modification the c_{n3} image is processed further to sharpen the selectivity according to Equation 1. This yields the image s_{n3} and the maximum in s_{13} and s_{23} image are found.

A window size of 13 x 13 is used when searching for the maximum responses in the next lower resolution s_{12} and s_{22} . The window size is empirically determined by tests. A point is accepted as an SP if a filter response s_{n2} has a value higher than a threshold, i.e. an acceptance of an SP is done at level 2. To improve the precision in position of the accepted SP the window procedure is applied to resolution level 1.

The argument of the complex filter response is computed as an average weighted argument using



Figure 6: Fingerprints in the visual inspection. Left: $s_{12} = 0.70$ and $s_{22} = 0.66$. Right: $s_{12} = 0.60$ and $s_{22} = 0.30$. (1 represents max certainty)

level 3 and level 2 according to:

$$\theta_n = \arg(\langle w_{n2}(x, y), c_{n2}(x, y) \rangle + \langle w_{n3}(x, y), c_{n3}(x, y) \rangle) \quad (5)$$

$$w_{nk}(x, y) = \frac{|c_{nk}(x, y)|}{\sum_{x, y \in L} |c_{nk}(x, y)|} \quad (6)$$

The symbol \langle, \rangle represents the 2D scalar product defined in the 3×3 neighbourhood around the maximum filter responses. The same 3×3 area called L is utilized to obtain w_{nk} via the normalization in Equation 6. The weighting in Equation 5 and 6 favours arguments belonging to strong filter responses compared to arguments belonging to weaker filter responses in the 3×3 neighbourhood L.

5.2 Position of symmetry points

Due to the fact that the true position of the SPs in the fingerprint are not known, we were obliged to do a visual inspection of the positions of the estimated SPs for each fingerprint in the database. A total of 800 fingerprints were inspected. In each fingerprint the position of the maximal filter response in level 2 for each type of SP (core, delta) has been noted. Here core type is marked with a square, and a delta type with a cross. Also, the certainty measure s_{n2}

FVC2000 database. 800 fingerprints	Core No.	Core %	Delta No.	Delta %
False singular point (FA).	41	5.1	18	2.3
Missed singular point (FR).	46	5.8	23	2.9

Table 1: Results of recognition

for the maximal filter response of the two types (core $n = 1$, delta $n = 2$) is printed out. Figure 6 shows examples of images in the visual inspection.

If the certainty measure is higher than a threshold T the point is classified as an SP. If the position is incorrect despite that the certainty is high the point is classified as a "False singular point". This case is a false acceptance case (FA).

If the certainty measure is lower than a threshold T the point is classified as being not an SP. If the point is despite that an SP and its position is correct, the point is classified as a "Missed singular point". This is in other words a false rejection (FR) of an SP.

The classification of core points is done by using a threshold value of $T_1 = 0.45$. In the classification of delta points $T_2 = 0.5$ is used. This choice was made to reach approximately Equal Error Rate (EER). EER is a standard measure widely utilized to quantize the performance of recognition systems. "All" thresholds are tried out but only those yielding EER are reported to quantify FA and FR curves with one number. The overall result is presented in Table 1.

The relative high number of misclassification of core points can be tracked to the same global structure of a fingerprint, namely plain arch (FBI's classification scheme [1]), see Figure 7 left. For this failing structure both filters give strong responses, and therefore low certainty measures are attained when using the selectivity rule (Equation 1). Also, there is a spatial spread out of strong filter responses compared to the tented arch structure which gives an uncertainty in the position. A border problem also exists, i.e. the border between the background and the fingerprint generates strong responses in the ori-



Figure 7: Left: Missed singular points: $s_{12} = 0.40$ $s_{22} = 0.40$. Right: False singular point, cross: $s_{12} = 0.65$ $s_{22} = 0.60$.

entation tensor image and therefore "False singular points", see Figure 7 right.

In the experiment we only use one certainty measure (maximal filter response from one of the filters) to classify the point being an SP or not. Instead we could represent each point by its feature vector, where the features are the responses from both filters. The feature vector can then be used to classify each point as an SP or not, and also which type of SP it is.

5.3 Orientation of symmetry points

The orientation of an SP is estimated from the argument θ_n of the complex filter responses according to Equation 5. For a core point the orientation is estimated by $\theta_{core} = \theta_1$ and for a delta point by $\theta_{delta} = \frac{\theta_2}{3}$ [11].

To find out the error in the orientation estimate a fingerprint is rotated -50° to 50° in steps of 2° . For each rotation step the rotation angle is obtained by estimating SP position and orientation as in a new image. The change in orientation is calculated by taken the angle difference between the SP in the original fingerprint (0° rotation) and the extracted SP in the rotated fingerprint. The result of the test is plotted as in Figure 8. An ideal result of the orientation estimate is a line with an inclination angle of 45° .

Figure 8 and 9 shows orientation estimates for the marked SPs in the fingerprint images to the left of the plot. In Figure 8 the mean error respectively the standard deviation of the orientation estimate is $mean = -1.1^\circ$ and $std = 2.6^\circ$ for the core point. For the delta point $mean = 0.2^\circ$ and $std = 0.4^\circ$. Figure 9 indicates a robustness in the orientation estimate.

Tests on several fingerprints that we have done show similar results as those illustrated here. In conclusion these experiments reveal that an unbiased orientation estimate with a standard deviation of less than 4° can be achieved by using the argument of the complex filter response belonging to an SP. Bazen and Gerez [8] report a standard deviation of 12° in the orientation estimate.

5.4 Alignment

To test the precision of the alignment process with the automatically obtained rotation and translation parameters we have, for a person in the database, manually chosen one fingerprint as the reference fingerprint and the other seven as test fingerprints. In the reference fingerprint the coordinates of an arbitrary minutia point (occurring in all 8 images!) is manually identified including their coordinates. It should be noted that these minutiae are different than the SPs which are automatically identified by the method proposed here, and the manual identification is for the purpose of quantification of errors in the alignment process. It gives a total of 371 test samples (originating from 53 persons, $371=53 \times 7$) for the alignment.

An SP of type core is more often positioned in the middle of a fingerprint compared to an SP of type delta. Because we want to choose the minutiae in a way that angles and distances around an SP became approximately uniformly distributed only SPs of type core are used in the estimation of the alignment parameters φ and v . This is the worst case, because the pattern of a delta point is more suitable for orientation estimation compared to the pattern of a core point due to lower errors, see Figure 2. This is also confirmed in the orientation estimate test in Section 5.3.

Several tests were done to find out from which res-

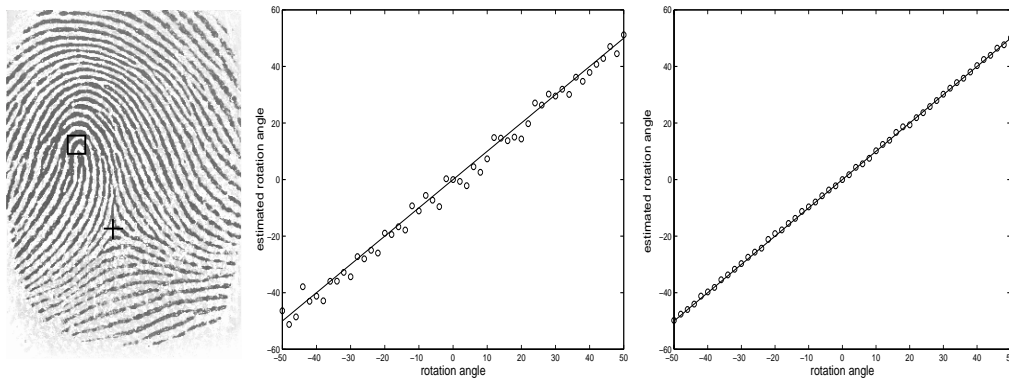


Figure 8: Middle: orientation estimate for a core point ($mean = -1.1^\circ$, $std = 2.6^\circ$). Right: orientation estimate for a delta point ($mean = 0.2^\circ$, $std = 0.4^\circ$).

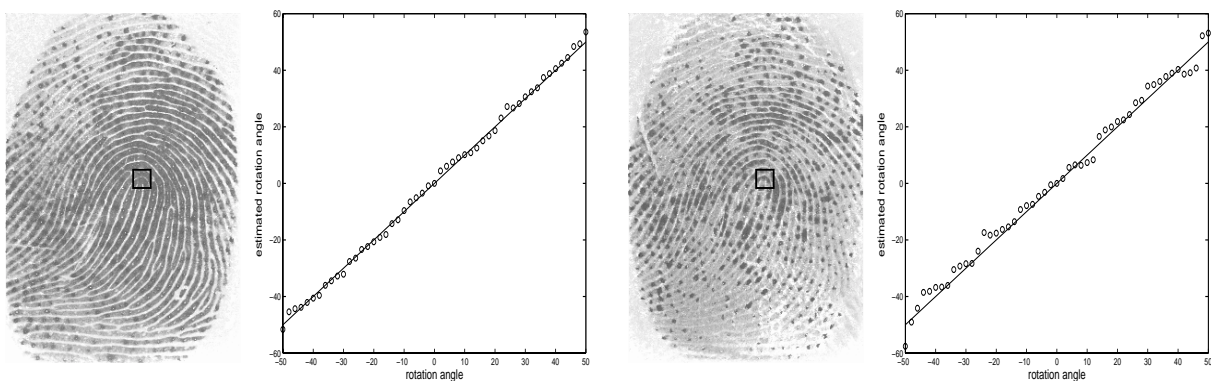


Figure 9: Orientation estimates for core-points (Left: $mean = 0.3^\circ$, $std = 1.3^\circ$. Right: $mean = 1.1^\circ$, $std = 2.7^\circ$).

olution level k the complex filter responses should be chosen to give the optimal alignment result. Generally one can say that the rotation parameter φ should be estimated from higher levels (low resolution), and the translation parameter v should be estimated from lower levels (high resolution). This is expected since the uncertainty principle in image analysis stipulates that position and property precisions can not be improved simultaneously [20].

The result presented in Table 2 has been reached by using level 3 and level 2 for the rotation angle estimation (Equation 5), and resolution level 1 for the translation parameter estimation.

FVC2000 database. 371 fingerprints.	Mean in pixel	Stand. deviation in pixel
Row direction	-0.66	10.7
Column direction	-0.35	7.0

Table 2: Results of alignment

Figure 10 shows the histogram of the error in the alignment process. The error is computed as: $e = p' - p_{correct}$. p' is computed from Equation 2, and $p_{correct}$ is the coordinates of the manually identified minutia point in the test fingerprint. When computing p' , p is the manually identified minutiae point in

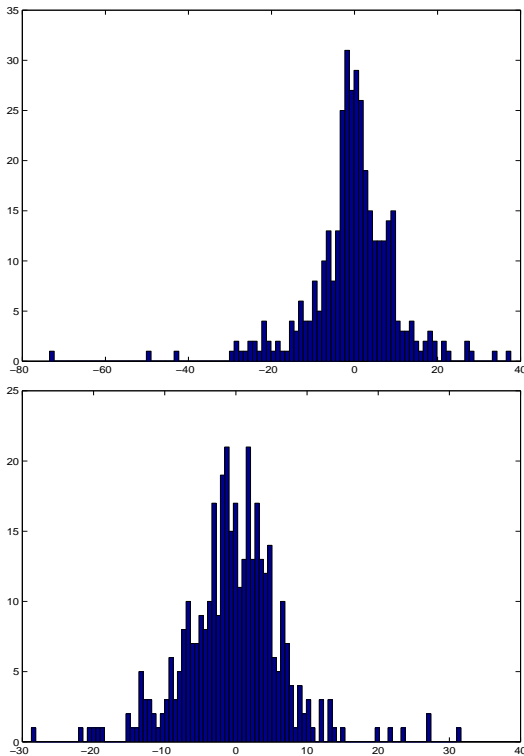


Figure 10: Top: the histogram for the error in the row direction. Bottom: the histogram for the error in the column direction.

the reference fingerprint, and p_{rot} is the position of the SP in the reference fingerprint. The alignment parameters φ and v are estimated from the SPs in the reference and the test fingerprint.

The standard deviation σ_{row} in the row direction is 3% of the image height, and the standard deviation σ_{col} in the column direction is 3% of the image width. Compared to the wavelength of the fingerprint pattern the standard deviation of the errors are approximately the size of the average wavelength in the database.

In the alignment process there are some outlier errors. One such error is $e = (-73, 24)^t$ for the fingerprints shown in Figure 11. A large error is obtained for these two fingerprints because the position of the core point in the test fingerprint is badly estimated,

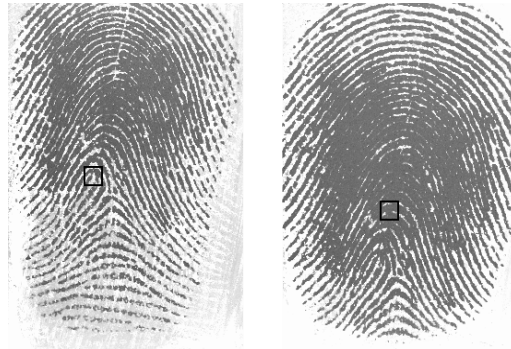


Figure 11: Left: reference fingerprint. Right: test fingerprint. Large error in the alignment due to wrong core point position in the test fingerprint.

which is a result of the very poor quality of the test fingerprint. This image can be avoided altogether by rejecting the area of low orientation certainty in the search for SPs.

We are not aware of other researchers who have attempted to quantify localization of corresponding points. For this reason it has not been possible for us to provide comparative results on alignment in this paper.

6 Conclusion

Given the difficulty level of the used database the results reported in this paper are, we believe, very encouraging for implementing a fully automatic fingerprint verification scheme.

The alignment test shows that the uncertainty (one standard deviation) in distance between two corresponding points is $\sqrt{10.7^2 + 7^2} \approx 13$ pixels.

This is confirmed by the uncertainty (one standard deviation) of less than $4^\circ \approx 0.07$ radians in the orientation estimate. The uncertainty in the rotation parameter φ (the difference of two estimated orientations) is then ≈ 0.1 radians. If we assume that the translation parameter is free from error (correct estimation of position) and the mean distance between an SP and a manually chosen minutiae point is 100

pixels an uncertainty of 0.1 *radians* in the rotation parameter gives an uncertainty in distance between two corresponding points of 10 pixels (compared to 13 pixels in the alignment test).

The empirical assumption of a mean distance of 100 pixels is motivated by the fact that the minutiae points were manually chosen in a way that angles and distances around an SP became approximately uniformly distributed, the SPs were frequently in the centre of the fingerprint, and the fingerprints were of size 364 x 256 pixels.

In this work we have used a modified filter response at level 3 according to Equation 4 to avoid poor quality fingerprint areas when searching for SPs. To better handle outliers (see Figure 11) more complex strategies to decide if an area should be rejected in the search for an SP will have to be used. The orientation certainty, i.e. the magnitude of the complex orientation field, is, we believe, a good parameter to use in this decision.

Only filters that detect parabolic symmetry patterns (rotational symmetries of order 1) have been used in this work because these patterns are similar to patterns of a core respectively a delta point. Future work includes the use of filters that extract other symmetries as well. To describe a point in a fingerprint a feature vector would be generated. The elements of such a vector are the responses to filters of different order of symmetries. This "symmetry representation" of a fingerprint, we believe, can be used to both align and match fingerprints even when a fingerprint pattern has no strong SPs.

Acknowledgment

This work has been possible by support from the swedish national SSF-program VISIT. We thank Bjorn Johansson, Linkoping University, for helping to generate Figure 2. We also thank the reviewers for their constructive criticisms.

References

- [1] R. Capelli, A. Lumini, D. Maio, and D. Maltoni. Fingerprint classification by directional image partitioning. *IEEE Transactions on Pattern Analysis and Machine Intelligence*, 21(5):402–421, May 1999.
- [2] J. Bigun and G. H. Granlund. Optimal orientation detection of linear symmetry. *IEEE Computer Society Press, Washington, DC*, pages 433–438, June 1987. In First International Conference on Computer Vision, ICCV (London).
- [3] K. Karu and A. K. Jain. Fingerprint classification. *Pattern Recognition*, 29(3):389–404, 1996.
- [4] A. K. Jain, S. Prabhakar, L. Hong, and S. Pankanti. Filterbank-based fingerprint matching. *IEEE Transactions on Image Processing*, 9(5):846–859, May 2000.
- [5] J. Van de Weijer, L. J. van Vliet, P. W. Verbeek, and M. van Ginkel. Curvature estimation in oriented patterns using curvilinear models applied to gradient vector fields. *IEEE Transactions on Pattern Analysis and Machine Intelligence*, 23(9):1035–1042, September 2001.
- [6] M. K. Koo and A. Kot. *Curvature-based singular points detection*. Springer LNCS 2091. Springer Bigun Smeraldi Eds, 2001. Third International Conference AVBPA 2001, Halmstad, Sweden.
- [7] M. Kawagoe and A. Tojo. Fingerprint pattern classification. *Pattern Recognition*, 17(3):295–303, 1984.
- [8] A. M. Bazen and S. H. Gerez. Systematic methods for the computation of the directional fields and singular points of fingerprints. *IEEE Transactions on Pattern Analysis and Machine Intelligence*, 24(7):905–919, July 2002.
- [9] J. Bigun. Recognition of local symmetries in gray value images by harmonic functions. *Ninth International Conference on Pattern Recognition, Rome*, pages 345–347, 1988.

- [10] J. Bigun, G. H. Granlund, and J. Wiklund. Multidimensional orientation estimation with applications to texture analysis and optical flow. *IEEE Transactions on Pattern Analysis and Machine Intelligence*, 13(8):775–790, 1991.
- [11] J. Bigun. Pattern recognition in images by symmetries and coordinate transformations. *Computer Vision and Image Understanding*, 68(3):290–307, December 1997.
- [12] H. Knutsson, M. Hedlund, and G. H. Granlund. Apparatus for determining the degree of consistency of a feature in a region of an image that is divided into discrete picture elements. *US Patent, 4.747.152*, 1988.
- [13] J. Bigun and T. Bigun. Symmetry derivatives of gaussians illustrated by cross tracking. *Research report IDE-0131*, September 2001.
- [14] W. Rudin. *Real and complex analysis*. Mc. Graw-Hill, New York, 1987.
- [15] G. Drets and H. Liljenstrom. Fingerprint subclassification and singular point detection. *International Journal of Pattern Recognition and Artificial Intelligence*, 12(4):407–422, June 1998.
- [16] B. Johansson. *Multiscale curvature detection in computer vision*. Tech. lic., Linkoping University, Linkoping University, Dep. Electrical Eng., SE-581 83, 2001.
- [17] V. Govindu and C. Shekhar. Alignment using distributions of local geometric properties. *IEEE Transactions on Pattern Analysis and Machine Intelligence*, 21(10):1031–1043, October 1999.
- [18] G. H. Granlund. In search for general picture processing operator. *Computer Graphics and Image Processing*, 8(2):155–173, October 1978.
- [19] D. Maio, D. Maltoni, R. Cappelli, J. L. Wayman, and A. K. Jain. Fvc2000: Fingerprint verification competition. *IEEE Transactions on Pattern Analysis and Machine Intelligence*, 24(3):402–412, March 2002.
- [20] R. Wilson and G. H. Granlund. The uncertainty principle in image processing. *IEEE Transactions on Pattern Analysis and Machine Intelligence*, 6(6), November 1984.